*32nd EPS Conference on Plasma Phys. Tarragona, 27 June - 1 July 2005 ECA Vol.**29C**, P-1.113 (2005)*

Modelling of Rotating Plasma States under the Influence of Helical Perturbations

A. Nicolai[1], U. Daybelge[2], C. Yarim[2]

[1]*Institut für Plasmaphysik, Forschungszentrum Jülich GmbH, Euratom Association, Trilateral Euregio Cluster, D-52425 Jülich, Germany*

[2]*Istanbul Technical University, Faculty of Aeronautics and Astronautics, 80626 Maslak, Istanbul, Turkey*

Abstract

The parallel and poloidal rotation speeds are calculated on the basis of the ambipolarity constraint and the parallel momentum equation of the revisited neoclassical theory. The temperature is estimated by means of the power balance. Source terms account for the momentum deposition by neutral beam injection, the eddy currents in the wall, pressure anisotropization and the $\vec{j}\times\vec{B}$ force density.

The main results are: (1) At a DED (TEXTOR) frequency of 10 kHz a toroidal velocity gradient of 1.2 10^6 1/sec may be achieved and thus an ITB be generated. (2) The (sub-neoclassical) pressure pedestal in a (rotating) medium size H - mode plasma may be stabilized against the ballooning-peeling instability by ergodization.

Introduction

Anomalous plasma transport much below the neoclassical prediction is a key issue in fusion research. Therefore the surprising experimental discovery of the transition to a high confinement mode above a certain heating power has evoked considerable interest in improved confinement regimes which seem to be related to toroidal and/or poloidal plasma spin up and the rise of (sheared) radial electric fields, both described by the 'revisited' neoclassical theory [1]-[3].

Plasma rotation and power balance

The main result of the revisited neoclassical theory [3] are the equations describing the radial transport of toroidal and poloidal momentum in a collisional subsonic plasma with steep gradients. A third equation stands for the power balance [4].

$$\frac{1}{\eta_2}\frac{\partial}{\partial x}(\eta_2 G) = \frac{\partial}{\partial t_T} g + T_{CX} + T_{NBI} + T_{ANI} + T_{j\times B} + T_{wall} \qquad (1)$$

$$(1+2q^2)\frac{\partial h^\star}{\partial t_P} = -(h^\star+1.833)M_1^2\gamma + \{\frac{0.45\Lambda M_1}{1+Q^2/S^2}\tilde{\nu}_T[-\frac{B_\phi}{B_\theta}]^2\{\frac{0.107q^2}{1+Q^2/S^2}h^\star + \frac{1}{2}\frac{1}{[\frac{\partial\hat{T}}{\partial x}]^2}(g^\star)^2 - \frac{1}{\frac{\partial\hat{T}}{\partial x}}g^\star[h^\star-(1+\frac{2}{\eta})] + 1.9[h^\star-0.8(1+\frac{1.6}{\eta})]^2\}\} \quad (2)$$

$$-\frac{1}{r}\frac{\partial}{\partial r}[-(R_n\chi_e+\chi_i)n\frac{\partial T}{\partial r} + C_V(T_e\Gamma_e+T_i\Gamma_i] + P_{OH}+P_{NBI}+P_{rad} = 0 \quad (3)$$

The quantity G in equation (1) is defined by $G = \frac{\partial g}{\partial x} - M_1\frac{0.107q^2}{1+Q^2/S^2}\frac{\partial ln\,T}{\partial x}\frac{B_\phi}{B_\theta}h$ g and h are the normalized toroidal and poloidal velocities T_{CX}, T_{NBI}, T_{ANI}, $T_{j\times B}$, T_{wall} account for the friction caused by the neutral gas, the momentum source due to neutral beam injection, the braking due to pressure anisotropization evoked by helical perturbation fields, the force density due to the $\vec{j}\times\vec{B}$ force at the singular layer and the force density due to the eddy currents in the wall which are induced by the currents in the singular layer [3], respectively. Analogously, in the power balance (3) P_{OH}, P_{NBI}, P_{rad} account for ohmic heating, neutral beam injection and radiation. $x = \frac{r-r_{in}}{L_\psi}$ is the radial coordinate. The normalized time variables are $t_P = \frac{t}{t_{cp}}$ and $t_T = \frac{t}{t_{ct}}$. R, B_θ, B_ϕ, q, $\chi_{e,i}$, Ω_j are 'selfexplanatory', the (effective) radius r, the 'inflection' radius r_{in}, the temperature decay length L_ψ, the characteristic times t_{cp} and t_{ct}, the ratio η, the velocities Q, S, $\tilde{\nu}_T$, the perpendicular viscosity coefficient η_2, the metric quantities M_j and γ, the relative quantities $\hat{T} = \frac{T}{T_{in}}$, $\hat{n} = \frac{n}{n_{in}}$ and $\hat{\eta}_2 = \frac{\eta_2}{\eta_{2in}}$ are defined in [3]. The quantities $g^\star$ and $h^\star$ have a normalization different from that of g and h to cast equation (2) which is an algebraic equation for $h^\star$, into a convenient form. The parameter Λ (crucial in the case of ALCATOR where finite Larmor radius effects are important) can be written as $\Lambda = \frac{\nu_j}{\Omega_j}\frac{q^2R^2}{L_T r}$. L_T is defined in [3], ν_j is the ion - ion collision frequency. The characteristic time t_{cp} for the evolution of $h^\star$ is considerably smaller than t_{ct} for the evolution of g. This allows to assess the stability of the solution by means of a two time step analysis.

Three approaches to the heat diffusivity $\chi_t = R_n\chi_e+\chi_i$ were used in attempting to reproduce the temperature profile in ALCATOR C-MOD and to predict the temperature profile in a generic medium size divertor device [4]. In the first two the 'subneoclassical' dependence ($\chi_{neo} = \kappa_0[1+1.6\frac{q^2}{1+\frac{Q^2}{S^2}}]\nu_i r_{ci}^2$) in the pedestal region is assumed. In the central core (1) a parabolic depence or (2) the dependence obtained by inverting the experimental temperature profile is used ($\chi_{t_{1,2}}$). As third option (as a check) the inverted heat diffusivity profile is applied everywhere (χ_{t_3}). This reproduces the experimental profile (Fig. 1).

Results

The TEXTOR (shot # 91269) input data are: $r_{in} = r_s$=46 cm, R=175 cm, $n_{max} = 5.4\,10^{13} cm^{-3}$, η=1.6, B_ϕ = 2.23 T, I_p = 350 kA. Fig. 2 shows the temperature profile. NBI is characterized by P_{MW} = 0.72, E_{keV} = 40 (deuterons).

By gradually increasing the rotation speed of the helical field at low slip frequency [3] to Ω_f=10 kHz, a local maximum can be produced at r=25 cm (Fig. 3). The gradient $\frac{dv_t}{dr}$ at r=40 cm is 1.2 10^6 $\frac{1}{sec}$ i. e. larger than required by the growth rate of the ITG [3]. We note that the plasma acceleration shown in Fig. 3 entails a strong increase of the central velocity, by around a factor two.

In Fig. 4 the power balance (3) is benchmarked with ALCATOR C-MOD data. We use χ_{t_2}, defined in the 2nd section. The temperature pedestal is reproduced with a high accuracy. This means that subneoclassical transport is reached in the pedestal.

The model is then applied to a generic medium size (divertor) tokamak. TEXTOR 'H-mode' plasmas are considered as well. Fig. 5 displays the L-mode temperature profile together with the H - mode profile evoked by the divertor by reducing the neutral gas influx thus increasing the velocity shear. In Fig. 6 the pedestal width is broadend from the width Δ=1 cm to Δ=2.5 cm because the radial extension of the ergodized region at the separatrix, produced by helical coils (like in TEXTOR) is of the order of 2 cm. Therefore ballooning - peeling stability may be achieved as it was shown at DIII-D, however, for a different (nonresonant) configuration. The recently investigated limiter 'H-mode' plasmas in TEXTOR (with pressure pedestal approaching the balloning limit mainly due to a reduction of the toroidal field) could be stabilized by means of the DED. This result which is still under discussion, seems to confirm the above considerations.

References

[1] A. L. Rogister, J. E. Rice, A. Nicolai, A. Ince - Cushmann, S. Gangadhara, Alcator C-Mod group, Nucl. Fus. 42 (2002) 1144

[2] U. Daybelge, C. Yarim, A. Nicolai, Nucl. Fus. 44 (2004) 966

[3] A. Nicolai, U. Daybelge, C. Yarim Nucl. Fus.44 (2004) S93 - S107

[4] A. Nicolai, U. Daybelge, Proceedings of the 29 EPS - conference, Montreux, 2002 paper P 1.052

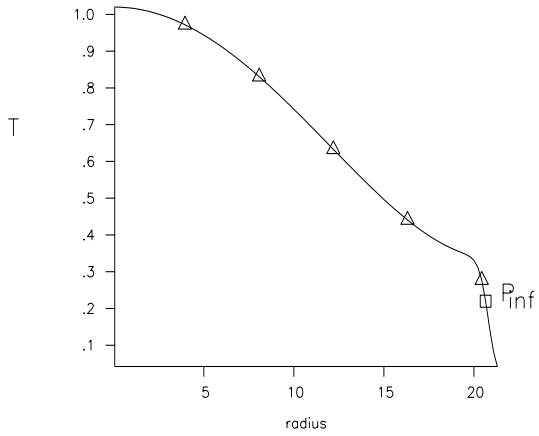

Figure 1: Ion temperature $T_i[keV]$ (ALCATOR) versus radius r[cm].

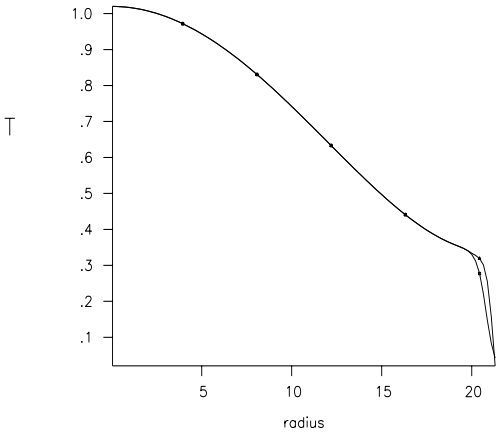

Figure 4: Computed (upper curve) and measured ion temperature in ALCATOR [keV]

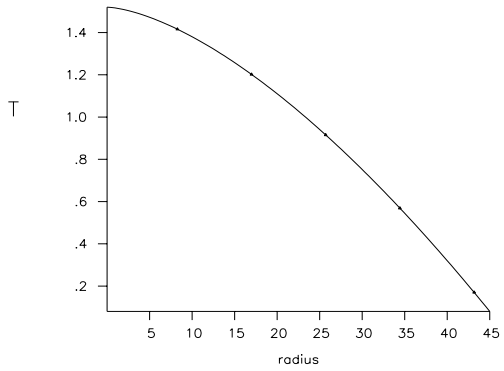

Figure 2: Ion temperature $T_i[keV]$ in TEXTOR versus radius r[cm].

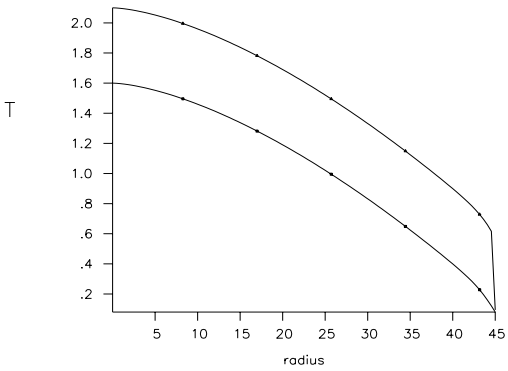

Figure 5: L- and H - mode temperatures in a medium size Tokamak versus radius r[cm].

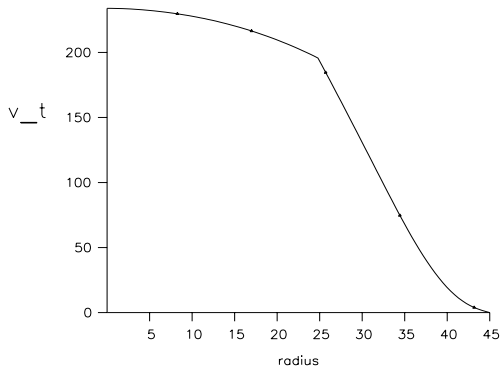

Figure 3: Toroidal speed v_t[km/sec] with rotating helical field (m=2, n=1) (TEXTOR).

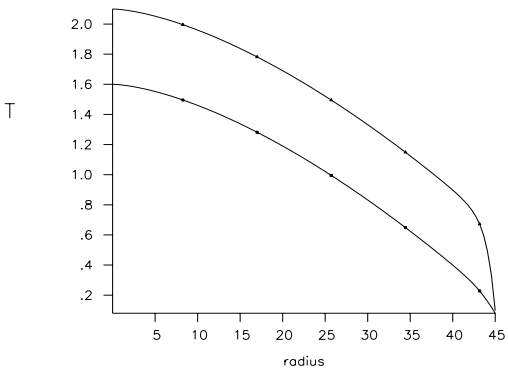

Figure 6: Ion temperature $T_i[keV]$ as in Fig. 5, however, with ergodized separatrix region.